

Application of High-Intensity Ultrasound to Palm Oil in a Continuous System

Yubin Ye and Silvana Martini*

Department of Nutrition, Dietetics, and Food Sciences, Utah State University, 8700 Old Main Hill, Logan, Utah 84322-8700, United States

Supporting Information

ABSTRACT: High-intensity ultrasound (HIU) was used in a continuous system to change the crystallization behavior of palm oil. Different power levels (75, 110, and 180 W) and pulse durations (continuous application and 5, 10, and 15 s pulses) were used to optimize sonication conditions. Results showed that HIU applied at low power level (75 W) was the most efficient condition in inducing palm oil crystallization at 35 °C, generating a crystalline network with higher solid fat content (SFC), higher elasticity, and sharper melting profile after 60 min of crystallization. Changes in elasticity observed as a consequence of sonication were maintained after tempering the samples at 25 °C for 24 h, but were lost after tempering at 5 °C. No significant differences ($\alpha = 0.05$) were observed in SFC values of the sonicated and nonsonicated samples after tempering, whereas the sharper melting behavior observed in the sonicated sample was maintained after tempering.

KEYWORDS: *high-intensity ultrasound, flow cell, power level, crystallization, palm oil, polymorphism*

INTRODUCTION

Power ultrasound, or high-intensity ultrasound (HIU), is an invasive technique that uses acoustic waves operating at low frequency (20–100 kHz) and high power (10–10000 W cm⁻²) levels. These acoustic waves travel through the material and induce the formation of cavities.¹ Cavitation is associated with high localized temperatures, high shear forces, and high pressures that lead to several physicochemical changes in the material.² Some of these changes include the generation of chemical reactions (sonochemistry),^{3,4} changes in crystallization behavior (sonocrystallization),^{5,6} and changes in physical properties of materials.^{7–9} In particular, sonocrystallization is defined as the phenomenon associated with the induction or modification of the crystallization behavior of different materials without generating any chemical changes.¹⁰ Sonocrystallization techniques have been used in food applications since the early 2000s. Chow et al. used HIU to modify the primary and secondary nucleation of ice and sucrose,^{11,12} whereas Patel et al. showed that power ultrasound can be used to control the crystallization process of lactose during the nucleation phase.¹³ Early studies in lipid systems were performed by Patrick et al., who evaluated the effect of ultrasonic intensity on palm oil crystalline structures.¹⁴ Sato and co-workers used HIU in cocoa butter and pure triacylglycerols^{15,16} and showed that HIU induces lipid crystallization as evidenced by shorter induction times in sonicated samples. In addition, these authors showed that HIU promotes the formation of a stable polymorphic form, especially at high crystallization temperatures.

Previous work in our laboratory^{17–20} and by other research groups²¹ indicates that HIU can be used as a novel processing tool to modify the functional properties of lipids. HIU has the ability to change the crystallization behavior of lipids and therefore their functional properties such as texture, thermal behavior, solid/liquid ratio, and crystal size.

All previous studies about lipid sonocrystallization have been performed in a batch with volumes between 5 and 100 mL.^{16–21} The effect of HIU on the crystallization of lipids in a continuous system has never been investigated.

The purpose of this research is to evaluate the use of HIU in a continuous system, which is a more realistic representation of an industrial setting. The overall objective of this research is to optimize the processing conditions (power level and irradiation pulse) needed to use HIU in a continuous system to modify the physical properties (microstructure, melting profiles, polymorphism, and viscoelasticity) of palm oil.

MATERIALS AND METHODS

Materials. Refined, bleached, and deodorized palm oil provided by Archer Daniels Midland (ADM Oils, Oils Division, Chicago, IL, USA) was used in this experiment. The melting point of the palm oil is 37.2 ± 0.4 °C (AOCS Official Method Cc 1-25). The chemical composition of the sample consisted of 48% of saturated fatty acids, 40% of monounsaturated fatty acids, 10% of polyunsaturated fatty acids, and 2% of *trans*-fatty acids according to the product data sheet provided by ADM.

Sample Preparation and Continuous System. The continuous system consisted of a flow cell connected to a sonicator and an external water bath (Figure 1). Five liters of palm oil was placed in a 6 L Erlenmeyer flask and melted in a 70 °C water bath to completely erase crystal memory. The flask was then placed in a 40 °C water bath to allow for temperature stabilization. Once the sample reached approximately 42 °C, it was pumped into the flow cell at 7.3 mL/s using a peristaltic pump (261 mL; the retention of the sample in the cell is around 36 s) and collected in NMR tubes and beakers. The flow cell was connected to a water bath filled with an ethylene glycol water mixture (3:1 v/v) and set at -18 °C. This low temperature in the

Received: October 17, 2014

Revised: December 16, 2014

Accepted: December 17, 2014

Published: December 17, 2014

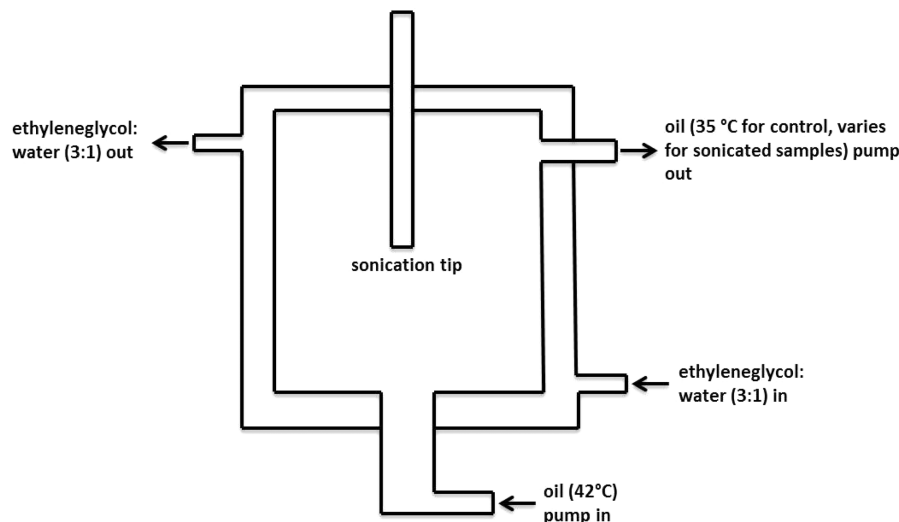


Figure 1. Flow cell system used to evaluate the effect of HIU on the crystallization behavior of palm oil.

water bath was necessary to cool the sample in the flow cell from 42 to 35 °C. A diagram of the flow cell used is shown in Figure 1.

Ultrasound Application. HIU (20 ± 1 kHz operation frequency) was generated using UIP1500hd equipment (Hielscher Ultrasound Technology, Ringwood, NJ, USA) with a 3.8 cm^2 frontal area sonication tip. HIU was applied 1 min after pumping of the sample had been started to ensure that the cell was completely filled with the sample and to stabilize the temperature of the sample. Previous research in our laboratory^{17,19} and by other research groups²¹ showed that the effect of HIU is more significant when samples are crystallized at low supercoolings. Because the melting point of our sample is 37.2 ± 0.4 °C, a crystallization temperature of 35 °C was chosen for our experiments. The effects of ultrasound using different power levels were evaluated in this study using 75 W (the lowest power setting that can be achieved by our ultrasound generator), 110 W (middle setting), and 180 W (safety maximum power setting recommended by the manufacturer of the sonicator). Sonication was applied in a continuous manner and using 5, 10, and 15 s pulse durations. A continuous duration indicates sonication continuously for 5 min, whereas sonication using an X s pulse duration means that HIU was applied every X s for a duration of X s. For example, a 5 s pulse duration means HIU was applied every 5 s with the duration of 5 s. Sample was pumped into the system for 5 min from the start of the sonication. Control samples (samples crystallized without the use of HIU) were collected at the beginning of the experiment before the application of HIU. Samples were collected every minute during the crystallization process in different tubes (one tube per minute). The first tube always consisted of nonsonicated sample (control). Solid fat content and crystal morphology were monitored in these samples as a function of storage time at 35 °C. Samples were kept at 35 °C in an incubator for 60 min to allow complete crystallization and then rapidly cooled to 25 and 5 °C and tempered for 24 h at these temperatures. The objective of this step is to evaluate if the effect of sonication is maintained through the tempering process.

Solid Fat Content (SFC). SFC values of palm oil during and after crystallization at 35 °C were measured using a NMR 120 minispec NMR analyzer (Bruker, Germany) following AOCS direct method Cd 16b-93. Samples were collected at the exit of the flow cell and loaded into the NMR tube every minute and kept at 35 °C to allow complete crystallization. SFC was measured as soon as the sample was taken out of the flow cell (time zero) and every 5 min for 30 min and every 10 min until the end of crystallization (60 min). The crystallization curves were fitted to the Avrami equation (eq 1) by least-squares nonlinear regression.²²

$$\text{SFC}_{(t)} / \text{SFC}_{(\infty)} = 1 - \exp(-kt^n) \quad (1)$$

$\text{SFC}(t)$ and SFC_{∞} are the SFC (%) at time t and the maximum SFC after crystallization is completed, respectively. The SFC data fitted to this model were used to determine the rate constant of crystallization (k) at a particular temperature and the mechanism of nucleation and crystal growth through the exponent, n .²³

Microstructure. Crystal morphology was recorded during crystallization using a polarized light microscope (PLM-Olympus BX 41 America Inc., Melville, NY, USA) with a digital camera (Lumenera Scientific, Infinity 2, Ottawa, Ontario, Canada) attached and a thermostated stage to allow for temperature control during the measurement. The pipet, slides, and slide covers were tempered at 35 °C in the incubator. A 20X magnification objective was used.

Crystal Polymorphism by X-ray Diffraction (XRD). After 60 min of crystallization, samples were filtered under vacuum for 2 min, and crystals were collected to perform XRD measurement. The same filtration treatment was performed in samples tempered at 25 and 5 °C for 24 h. Samples were filtered to separate as many crystals as possible from the liquid phase, minimize the signal of the liquid fat in the XRD, and therefore obtain a better resolution. The polymorphic forms of fat crystals were determined by using a Philips Analytical X'Pert Pro X-ray Diffraction system (PW 3040/60 Console). The X-ray generator used a high-power ceramic diffraction X-ray tube with copper anode (PW 3373/00 ceramic tube Cu LFF), with voltage at 45 kV and current at 40 mA. Samples were scanned from 3° to 30° (2θ scale) at a rate of $1^\circ/\text{min}$ at ambient temperature. The data were collected using X'Pert Data Collector and analyzed by X'Pert HighScore PANalytical software.

Melting Profile. The thermal behavior of the crystallized material was evaluated using a differential scanning calorimeter (DSC-TA Instruments Q20). The crystallized material (5–15 mg) was placed in a hermetic aluminum pan and heated from T_c (35, 25, or 5 °C) to 80 °C at 5 °C/min to evaluate its melting behavior. Melting parameters such as onset temperature (T_{on} ; temperature at which the sample starts melting), peak temperature (T_p ; temperature at which the melting peak reaches its maximum), and melting enthalpy (energy required for melting) were recorded. The melting enthalpy was used to evaluate the amount of crystallized material and the solid/liquid ratio in the lipid network. These analyses provided information about (a) the amount of solids generated as a consequence of HIU (induction or delay of the crystallization) through the melting enthalpy values, (b) the solid/liquid ratio of the crystal network formed as a function of temperature during melting, and (c) the melting range of the lipid network (through T_p and T_{on}).

Viscoelastic Properties. A TA Instruments AR-G2 magnetic bearing rheometer was used to evaluate the viscoelastic properties of the material. Oscillatory tests were performed by strain sweep step to obtain viscoelastic parameters such as the storage modulus (G'). The

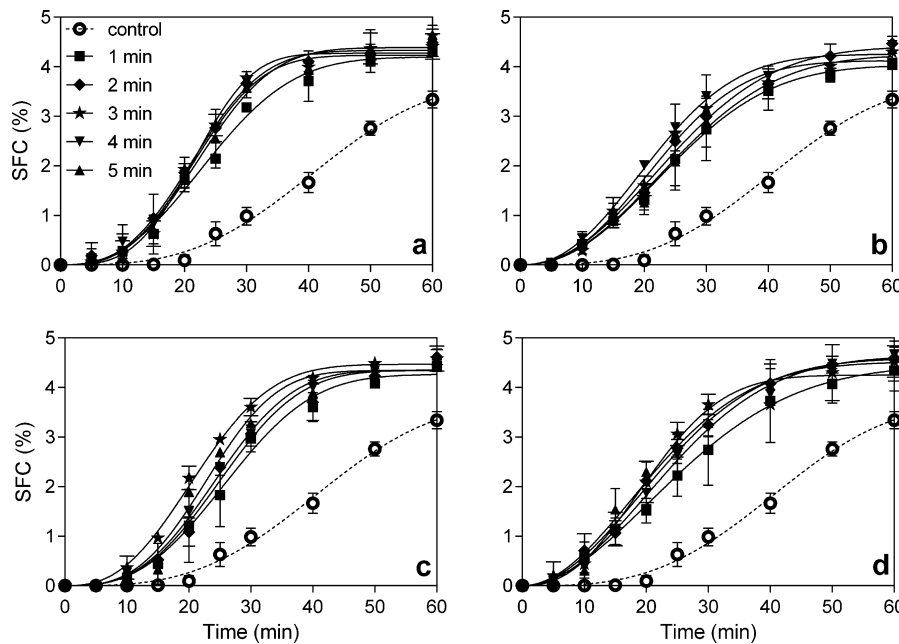


Figure 2. SFC of palm oil without (control, open circles) and with (solid symbols) HIU during the first 60 min of the crystallization process at 35 °C. A 75 W power level was used in a continuous manner (a) and using pulses of different durations (5, 10, and 15 s; b, c, and d, respectively).

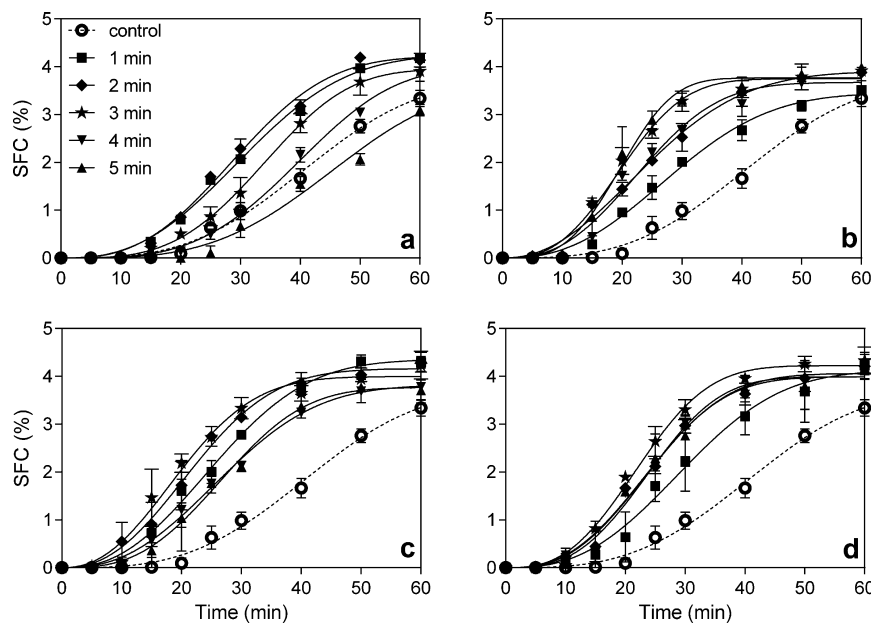


Figure 3. SFC of palm oil without (control, open circles) and with (solid symbols) HIU during the first 60 min of the crystallization process at 35 °C. A 110 W power level was used in a continuous manner (a) and using pulses of different durations (5, 10, and 15 s; b, c, and d, respectively).

experiments were carried out using a parallel plate geometry (40 mm diameter) with a temperature-controlled Peltier plate. The temperature of the plate was set at 35, 25, or 5 °C. For the strain sweep step, a constant frequency of 1 Hz (6.28 rad/s) was used, and strain values were set from 0.0008 to 10%.

Statistical Analysis. Crystallization experiments were performed in duplicate, and physical properties were measured in duplicate. Significant differences ($\alpha = 0.05$) were evaluated using two-way ANOVA using GraphPad Prism software, version 6.00 for Windows (GraphPad Software, San Diego, CA, USA).

RESULTS AND DISCUSSION

Optimizing the Process Condition. Figures 2–4 show the crystallization behavior of palm oil measured by SFC as a

function of time when different power levels of ultrasound were applied using different pulse types. Figure 2 shows SFC changes when samples were sonicated using 75 W power using a continuous sonication (Figure 2a), a 5 s pulse (Figure 2b), a 10 s pulse (Figure 2c), and a 15 s pulse (Figure 2d). When HIU is applied in a continuous manner, SFC values increased rapidly after 10 min, whereas SFC values increased after 20 min in the control samples (Figure 2a). Panels a–d of Figure 2 show no difference in crystallization between the modes of sonication (continuous vs pulses) with onset of crystallization observed at 20 min for the nonsonicated samples and at 10 min for the sonicated ones and final SFC values of 3.3 and 4.3% on average, Avrami analysis (R^2 values between 0.96 and 0.99)

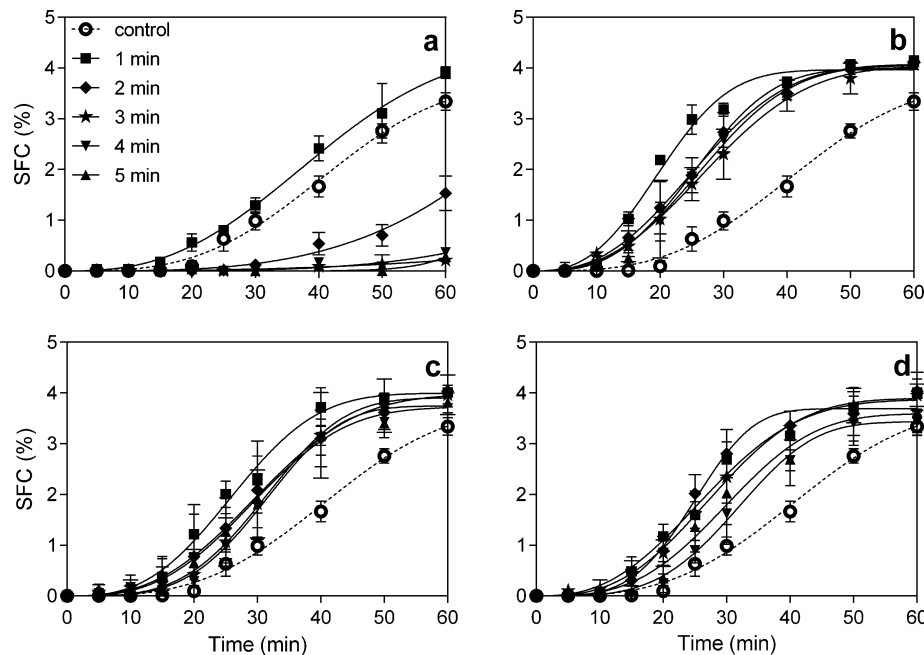


Figure 4. SFC of palm oil without (control, open circles) and with (solid symbols) HIU during the first 60 min of the crystallization process at 35 °C. A 180 W power level was used in a continuous manner (a) and using pulses of different durations (5, 10, and 15 s; b, c, and d, respectively).

showed 2 orders of magnitude higher k values for the sonicated samples compared to the nonsonicated ones with very little change in n values (Table 1). These data show that sonication indeed increased the crystallization rate of palm oil. Figure 3a shows SFC values obtained when samples were sonicated at 110 W in a continuous manner. This sonication condition did not induce lipid crystallization as shown by the similar SFC obtained between tubes at 1–5 min and the control tube and the similar values of k (Table 1). However, when sonication was applied using 5, 10, and 15 s pulses, sonication seems to be somehow efficient at inducing crystallization (Figure 3b–d) and k values were 1 or 2 orders of magnitude higher in the sonicated samples compared to the nonsonicated ones. R^2 values obtained from the Avrami fitting for these samples ranged between 0.96 and 0.99. When samples were sonicated using 180 W of power in a continuous manner (Figure 4a), HIU delayed crystallization after 2 min of sonication (see data in Figure 4a, tube 2 to 5 min). This delay in crystallization was so significant that data obtained for tubes 2–5 did not converge to the Avrami equation. Similar to the data discussed in Figure 3, HIU was able to induce crystallization when applied at 180 W using 5, 10, and 15 s pulses (Figure 4b–d), but higher k values were consistently obtained only for samples sonicated using 5 s pulses (Table 1). Avrami R^2 values ranged from 0.93 and 0.99.

Data obtained from the Avrami analysis show some variation in n values between the sonicated and nonsonicated samples (Table 1). n reflects details regarding nucleation and crystal growth mechanisms. Many studies discussed the values of n for various types of nucleation and growth of crystals.^{24,25} For example, an n value of 3 indicates plate-like growth from sporadic nuclei or spherulitic growth from instantaneous nuclei, whereas an n of 2 corresponds to needle-like growth from sporadic nuclei or plate-like growth from instantaneous nuclei. For the control samples, n values were close to 3, whereas after sonication, the n values decreased to close to 2. This suggests a change in the type of nucleation and growth of crystals after

HIU was applied. As discussed by Meng et al., lower values of n and higher values of k are associated with an increased rate of crystallization and a more instantaneous nucleation process with a shorter induction time.²⁵ Table 1 also shows the SFC_{∞} calculated using the Avrami fit with significantly ($P > 0.05$) higher SFC_{∞} values obtained for the samples sonicated using 75 W of power.

It is very likely that the lower efficiency of HIU observed at higher power levels is due to temperature increases obtained during sonication. When samples were sonicated in a continuous manner, a linear temperature increase was observed as a function of time with values of 0.6491 °C/min ($R^2 = 0.8879$) for 75 W, 1.463 °C/min ($R^2 = 0.9671$) for 110 W, and 1.847 °C/min ($R^2 = 0.9869$) for 180 W. The total temperature increases after 5 min of sonication are 3.2, 7.3, and 9.2 °C for 75, 110, and 180 W, respectively. The above results indicate that even though higher power levels of ultrasound can generate more cavitation in the system and therefore more positive effects on crystallization as described in previous research,^{19–21} they can also generate higher temperatures, which contrast the cavitation events by melting the crystals that are being formed. In this experimental setup, the thermal effect of higher power levels of HIU played an important role in delaying lipid crystallization (Figures 3a and 4a). In addition, greater temperature increases were obtained for the continuous application compared to the pulsed ones for samples sonicated at higher power levels (110 and 180 W). Temperature increases observed over the 5 min sonication using 110 W for 5, 10, and 15 s were 6.1, 4.9, and 6.2 °C, respectively, whereas temperature increases observed for the 180 W sonication condition were 5.8, 6.1, and 4.9 °C for the 5, 10, and 15 s pulses, respectively. The lower temperature increase for pulse irradiation types with higher power levels explains the induction in crystallization when pulse sonication was applied in Figures 3b–d and 4b–d. In summary, higher power levels of HIU generate more heat, and when the temperature is high enough, a delay in crystallization might occur. To overcome this

Table 1. Avrami Constant ($k, \text{ min}^{-n}$), Avrami Exponent (n^a), and Equilibrium or Maximum SFC (SFC_{∞,a}, %) Obtained from the Avrami Fitting for Samples Crystallized without and with Different Power Levels (75, 110, and 180 W) of Ultrasound

power	HIU	k_c	k_1	k_2	k_3	k_4	k_5
75 W	continuous	6.05×10^{-6}	2.3×10^{-4}	1.1×10^{-4}	1.6×10^{-4}	2.0×10^{-4}	1.8×10^{-4}
	5 s		5.8×10^{-4}	6.8×10^{-4}	4.8×10^{-4}	7.0×10^{-4}	6.0×10^{-4}
	10 s		7.4×10^{-5}	5.4×10^{-5}	2.6×10^{-4}	5.6×10^{-5}	5.0×10^{-5}
	15 s		1.3×10^{-3}	8.9×10^{-4}	2.0×10^{-4}	9.7×10^{-4}	8.7×10^{-4}
110 W	continuous		8.9×10^{-5}	6.2×10^{-5}	3.9×10^{-6}	1.6×10^{-6}	1.4×10^{-6}
	5 s		1.7×10^{-4}	6.4×10^{-4}	1.8×10^{-4}	1.9×10^{-4}	4.2×10^{-5}
	10 s		2.6×10^{-4}	4.8×10^{-4}	7.3×10^{-4}	1.9×10^{-4}	5.0×10^{-5}
	15 s		8.1×10^{-5}	1.5×10^{-4}	1.3×10^{-4}	5.8×10^{-5}	1.2×10^{-4}
180 W	continuous		4.4×10^{-5}				
	5 s		2.1×10^{-4}	1.5×10^{-4}	1.3×10^{-4}	7.3×10^{-5}	3.9×10^{-5}
	10 s		5.5×10^{-5}	5.0×10^{-5}	2.6×10^{-6}	1.4×10^{-6}	3.0×10^{-5}
	15 s		1.3×10^{-4}	3.4×10^{-6}	5.3×10^{-5}	1.6×10^{-6}	1.5×10^{-5}
power	HIU	n_c	n_1	n_2	n_3	n_4	n_5
75 W	continuous	3.14	2.53	2.84	2.75	2.66	2.65
	5 s		2.22	2.17	2.35	2.26	2.19
	10 s		2.80	2.93	2.58	2.95	3.04
	15 s		1.97	2.17	2.72	2.09	2.18
110 W	continuous		2.62	2.76	3.43	3.53	3.44
	5 s		2.49	2.19	2.75	2.61	3.25
	10 s		2.43	2.36	2.30	2.49	2.90
	15 s		2.67	2.66	2.77	2.95	2.73
180 W	continuous		2.65				
	5 s		2.71	2.61	2.59	2.79	3.02
	10 s		2.89	2.80	3.63	3.80	2.97
	15 s		2.61	3.81	2.86	3.77	3.16
power	HIU	SFC _{∞c}	SFC _{∞1}	SFC _{∞2}	SFC _{∞3}	SFC _{∞4}	SFC _{∞5}
75 W	continuous	3.70	4.20^b	4.33^b	4.31^b	4.26^b	4.41^b
	5 s		4.04	4.41^b	4.12	4.25^b	4.24^b
	10 s		4.26^b	4.35^b	4.47^b	4.35^b	4.34^b
	15 s		4.31^b	4.41^b	4.10	4.57^b	4.41^b
110 W	continuous		4.26^b	4.22	3.95	3.99	3.59
	5 s		3.45	3.91	3.75	3.67	3.77
	10 s		4.35^b	4.16	4.00	3.81	3.77
	15 s		4.12	4.06	4.23	3.99	3.99
180 W	continuous		4.34^b				
	5 s		3.96	4.07	4.04	4.05	4.00
	10 s		4.00	3.97	3.90	3.75	3.72
	15 s		3.87	3.69	3.90	3.43	3.60

^aSubscript “c” indicates the control sample, subscripts “1–5” indicate the samples collected at each minute during sonication. R^2 values for Avrami fitting were all above 0.96, except for the samples collected from 2 to 5 min under 180 W sonication in a continuous manner, where data did not fit the Avrami model. ^bSFC_∞ values are significantly different ($P < 0.05$) from the control sample.

disadvantage, pulse irradiation of sonication can be applied to induce crystallization by generating less heat. Temperature increases as a function of time can be found in Figure 1 of the Supporting Information.

Physical Properties of Sonicated Samples (75 W Continuous). Results described in the previous section demonstrate the sonication using 75 W is the most efficient at inducing crystallization and at generating more solids in the crystalline network formed. Because no differences were found in SFC values as a function of sonication mode (continuous vs pulse), the continuous mode was chosen to continue our

experiments of physical characterization of the sonicated samples. The continuous condition was chosen over the pulse ones because it would be an easier method to implement in a processing plant. To perform the physical characterization, samples were collected at the exit of the flow cell as described before and mixed together as the “sample with HIU”. A control sample was always taken before the sonication. Physical properties such as crystal microstructure, viscoelasticity, melting profile, and polymorphism were evaluated on these samples.

Microstructure of the Crystals. Figure 5 shows the microstructure of the palm oil samples crystallized in the flow

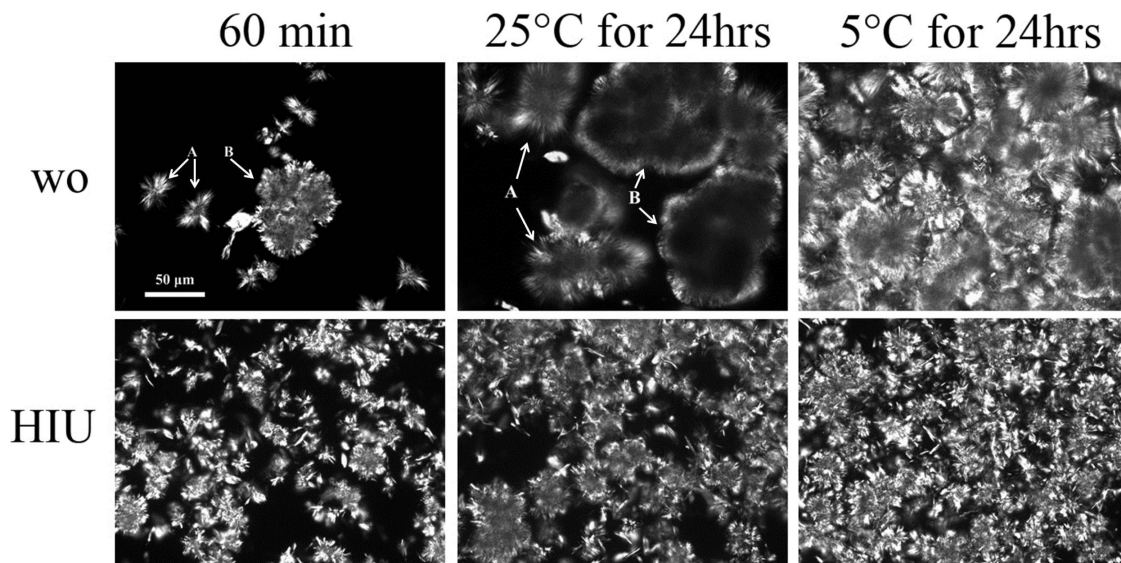


Figure 5. Microstructure of palm oil crystallized without and with HIU at 35 °C for 60 min and tempered at 25 °C for 24 h and at 5 °C for 24 h. In the pictures for samples without HIU for 60 min and at 25 °C for 24 h, two different morphologies are indicated (A and B).

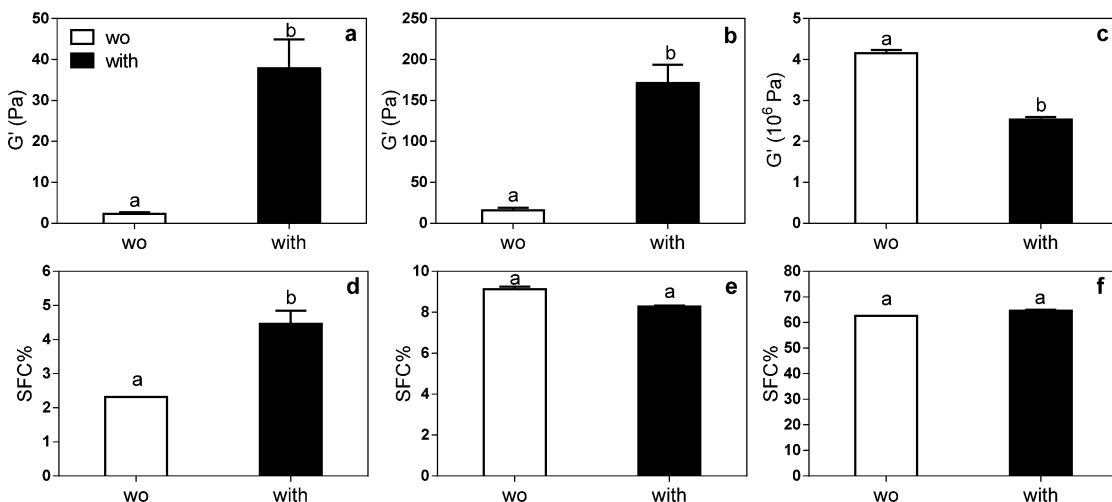


Figure 6. Storage modulus (G') and corresponding SFC values of palm oil crystallized without and with HIU at 35 °C for 60 min (a, d) and after tempering at 25 °C for 24 h (b, e) and 5 °C for 24 h (c, f).

cell with and without HIU using 75 W of power in a continuous manner. After crystallization had been induced in the flow cell, samples were kept at 35 °C in an incubator for 60 min to allow for complete crystallization and tempered for 24 h at 25 and 5 °C. PLM pictures shown in Figure 5 demonstrate that HIU significantly affects the formation of crystals in different sizes and shapes compared to the nonsonicated samples. Big round crystals (indicated with arrow B in the picture wo_60 min) were observed after 60 min at 35 °C in samples crystallized without HIU. A continuous growth of size for this big round crystal was observed after 24 h of tempering at 25 °C (approximately 80 μ m in diameter). Arrow A in the picture shows an example of a crystal with a different morphology characterized by needle-like spherulites, which are usually associated with β' crystals.²⁶ Crystals continued to grow and formed an interconnected crystalline network of big spherulites after tempering at 5 °C for 24 h, which makes the identification of individual crystals or clusters very difficult. When HIU was applied to the samples, the amount of crystal clusters increased and the crystal aggregates generated a more uniform size

distribution with smaller crystals, especially after 24 h of tempering. Similar results were found in the research on palm oil by Chen et al.,²¹ who showed different crystal morphologies of palm oil crystallized with and without sonication. It is also interesting to observe that crystal size and morphology did not change substantially in the sonicated samples as a function of tempering. There might be several reasons that can cause this phenomenon: (a) the greater number of crystals generated after HIU application act as nuclei for the secondary crystallization to occur, and therefore the solid mass deposited over each crystal is lower compared to the nonsonicated samples; (b) fewer crystals are present and therefore more solid mass is deposited in each crystal, resulting in crystal growth; (c) high pressures and high shear forces generated during sonication destroyed the regular shape of the crystal clusters and irregular or rough cluster shape might prevent the orderly arrangement of TAG molecules into the crystalline lattice.

Changes observed in crystal morphology as a consequence of sonication can be attributed to the formation of different molecular compounds or to the presence of different polymorphic forms. Therefore, XRD measurements were performed to evaluate the polymorphic forms generated during sonication and tempering.

Crystal Polymorphism. The polymorphism of crystals obtained after crystallization of the samples with and without HIU at 35 °C for 60 min was determined with X-ray. This measurement was also performed in the same samples tempered for 24 h at 25 and 5 °C. Signals at short spacings of 3.7, 3.8, 3.9, 4.45, and 4.6 Å were identified. All conditions tested showed a strong signal at 4.6 Å, indicating the presence of β crystals. No strong peaks were observed at 4.2 Å, indicating that β' crystals were not present in these samples^{27–30} (X-ray diffractograms can be found in Figure 2 of the Supporting Information).

Viscoelastic Properties. Figure 6 shows the comparison of the storage modulus (G') and the corresponding SFC measurements between samples crystallized with and without HIU application. Samples were taken after 60 min of crystallization at 35 °C and after 24 h of tempering at 25 and 5 °C. As expected, sonicated samples crystallized for 60 min at 35 °C had significantly ($P < 0.05$) higher G' and SFC values than those of nonsonicated ones. After 24 h of tempering at 25 °C, G' values for both samples (sonicated and nonsonicated ones) increased as a result of ongoing crystallization during tempering (Figure 5) due to the exposure to a higher supercooling. Sonicated samples maintained a higher G' after tempering ($P < 0.05$), whereas SFC values showed no statistical difference ($P > 0.05$). Changes observed in G' and SFC values after tempering at 25 °C might be due to different phenomena: (a) increased interaction between crystal clusters in smaller crystals (Figure 5), leading to a higher G' ; (b) SFC of the nonsonicated samples increased from 2.4 to 9.1% on average during tempering, whereas SFC of the sonicated samples increased only from 4.5 to 8.3%; this means that HIU induced the crystallization during the first 60 min and therefore there is not much left to crystallize during the tempering as the sample reached the thermodynamic equilibrium. When samples were tempered at 5 °C for 24 h, SFC values for both samples increased dramatically to the same level, and it is very interesting to observe that the G' values obtained for samples without HIU application are significantly higher than the ones obtained for the sonicated samples. The difference in crystal size and shape (Figure 5) and cluster interconnections might contribute to the different G' values observed after tempering at 5 °C for 24 h.

Melting Profile. The melting profiles of palm oil crystallized with and without HIU at 35 °C and stored at different tempering conditions (25 and 5 °C for 24 h) are shown in Figure 7. Only one melting peak was observed for both samples (with and without HIU) crystallized at 35 °C for 60 min (Figure 7a). Samples crystallized with HIU showed a sharper and deeper but narrower melting curve as compared to the nonsonicated sample. The peak temperature of the sample decreased from 48.4 ± 3.1 to 41.2 ± 0.1 °C when HIU was applied (Table 2). As expected, after tempering at 25 °C for 24 h (Figure 7b), two melting peaks were observed for both samples (with and without HIU). The melting peak observed at lower temperatures can be attributed to the secondary crystallization that occurred during tempering. Three peaks were observed for samples tempered at 5 °C for 24 h (Figure

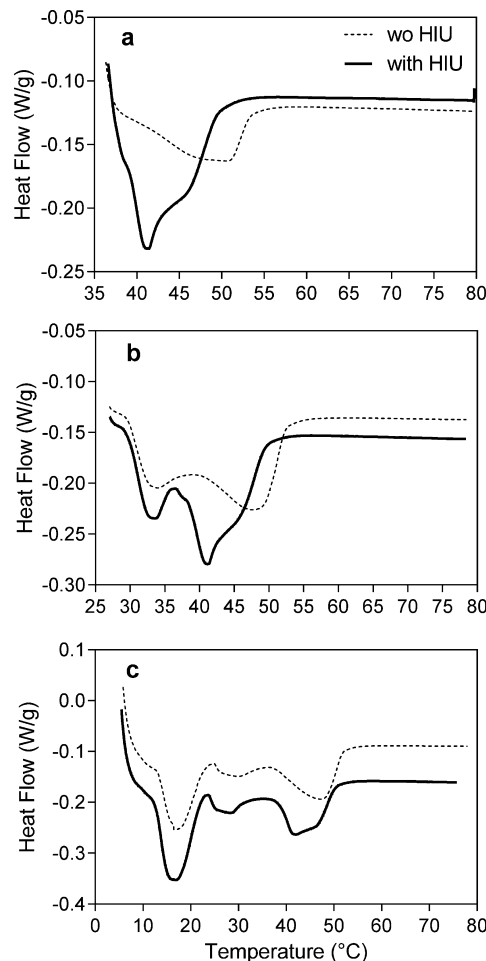


Figure 7. Melting profile of palm oil crystalline network obtained after crystallization without (dotted line) and with (solid line) HIU at 35 °C for 60 min (a) and after tempering at 25 °C (b) and 5 °C (c) for 24 h.

7c), of which the two lower melting peaks can be attributed to the secondary crystallization that occurs during the tempering at 5 °C. Table 2 shows the melting parameters of palm oil crystallized with and without HIU application. Melting parameters reported for the tempered samples correspond to the highest melting peak because this peak represents the crystals formed during the sonication experiment. The peak temperature (T_p) for the nonsonicated samples crystallized for 60 min at 35 °C was significantly ($P < 0.05$) higher than the sonicated samples. The same results were maintained after tempering at 25 and 5 °C for 24 h. The reason for the shift to lower peak temperature after sonication might be due to the different crystal microstructure and to different particle size distribution of the crystals. Enthalpy (ΔH) values of samples crystallized with HIU and kept for 60 min at 35 °C were significantly ($P < 0.05$) higher than the ones obtained in the nonsonicated samples. After tempering at 25 and 5 °C, no difference was found for the enthalpy between HIU samples with and without HIU for the highest melting fraction. These results are in accordance with previously discussed data related to SFC values (Figure 6).

Figure 8 shows the melting profile of the crystalline networks generated in this study. The melting profile is reported as the amount of solids remaining at a specific temperature (% solid) as the sample is being heated in the DSC. Only the highest

Table 2. Melting Parameters of Palm Oil Crystallized with and without Sonication^a

melting parameter	60 min		25 °C, 24 h		5 °C, 24 h	
	without HIU	with HIU	without HIU	with HIU	without HIU	with HIU
T_{on} (°C)	N/A	N/A	39.4 ± 0.9A	38.3 ± 0.5A	39.0 ± 1.6A	38.4 ± 0.0A
T_p (°C)	48.4 ± 3.1A	41.2 ± 0.1B	47.6 ± 1.5A	41.4 ± 0.1B	48.5 ± 1.1A	42.5 ± 0.3B
ΔH (J/g)	4.8 ± 0.4A	11.1 ± 0.6B	5.8 ± 0.3AC	6.8 ± 0.9AC	7.2 ± 1.9AC	9.4 ± 1.1BC

^aThe data were collected at 60 min and after tempering for 24 h at 25 and 5 °C. Data reported are mean values and standard deviations of two independent runs. The same upper case letters in a row indicate that values are not significantly different ($\alpha = 0.05$). N/A indicates that the value could not be calculated because it fell outside the temperature range of the DSC run.

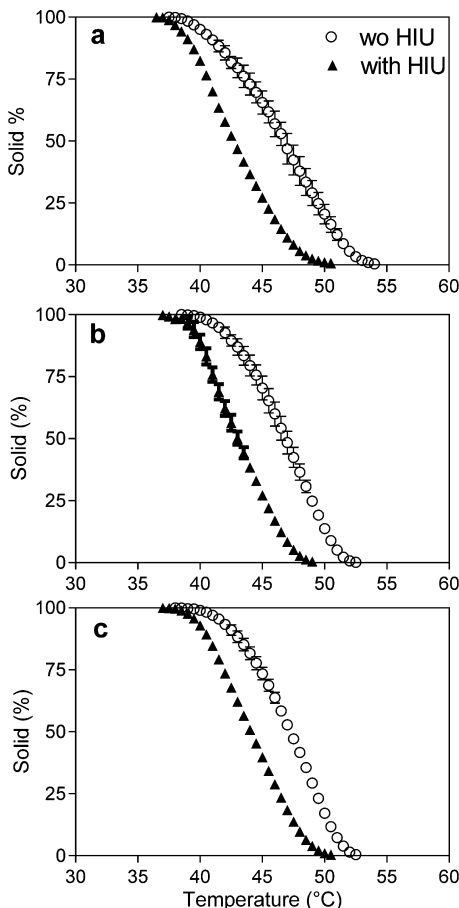


Figure 8. Melting profile of palm oil samples expressed as the percentage of solids remaining at a specific temperature during DSC melting. Melting profiles of sonicated and nonsonicated samples are indicated with solid and open symbols, respectively. Samples were crystallized at (a) 35 °C for 60 min and tempered at (b) 25 °C for 24 h and (c) 5 °C for 24 h.

melting fractionation was studied. Palm oil crystallized with HIU showed a lower percentage of solid at any given temperature when crystallized at 35 °C. The same results were maintained after tempering at 25 and 5 °C. The sonicated sample showed a steeper and sharper melting profile, which can be explained by the smaller size of crystals generated by HIU and as a consequence of a faster melting rate. Similar results were reported by Suzuki et al.¹⁸ and Ye et al.¹⁹ in other lipid systems such as anhydrous milk fat and interesterified soybean oil.

This study showed that HIU can be used in a continuous system to promote the crystallization of palm oil and to change its functional properties. Results obtained in this study provide scientific support to implement HIU as an additional

processing tool in the edible oil industry. The importance of optimizing the sonication conditions is highlighted in this research noting that the amount of heat generated during sonication can contrast the effect of cavitation. Future work in this area to support the hypothesis that HIU can be used as an additional processing tool to modify the functional properties of edible lipids in industrial settings could include changing the flow rate of the pumped oil and the crystallization temperature in the system. The goal of implementing this additional tool in the edible oil industry is not only to change the physical properties of the lipid but also to induce lipid crystallization, reduce processing times, and ultimately reducing processing costs.

ASSOCIATED CONTENT

Supporting Information

Figures 1 and 2. This material is available free of charge via the Internet at <http://pubs.acs.org>.

AUTHOR INFORMATION

Corresponding Author

(S.M.) E-mail: silvana.martini@usu.edu. Phone: (435) 797-8136. Fax: (435) 797-2179.

Funding

We thank the Utah Agricultural Experiment Station (UAES) (UTAO 1171 NC 1023) for funding support. This paper was approved by the UAES as Paper 8745.

Notes

The authors declare no competing financial interest.

ABBREVIATIONS USED

HIU, high-intensity ultrasound; AOCS, American Oil Chemists' Society; ADM, Archer Daniels Midland; NMR, nuclear magnetic resonance; SFC, solid fat content; PLM, polarized light microscopy; XRD, X-ray diffraction; DSC, differential scanning calorimetry; T_c , crystallization temperature; T_{on} , onset temperature; T_p , peak temperature; ΔH , enthalpy variation; G' , storage modulus; ANOVA, analysis of variance; n , Avrami exponent; k , Avrami constant; SFC_∞ , equilibrium solid fat content; TAG, triacylglycerol

REFERENCES

- Rastogui, N. K. Opportunity and challenges in application of ultrasound in food processing. *CRC Crit. Rev. Food Sci.* **2011**, *51*, 705–772.
- Soria, A. C.; Villamiel, M. Effect of ultrasound on the technological properties and bioactivity of food: a review. *Trends Food Sci. Technol.* **2010**, *21*, 323–331.
- Mason, T. J. Sonochemistry: current uses and future prospects in the chemical and processing industries. *Philos. Trans. R. Soc. London, A* **1999**, *357*, 355–369.

- (4) Suslick, K. S.; Mdleleni, M. M.; Ries, J. T. Chemistry induced by hydrodynamic cavitation. *J. Am. Chem. Soc.* **1997**, *119*, 9303–9304.
- (5) de Castro, M. D. L.; Priego-Capote, F. Ultrasound-assisted crystallization (sonocrystallization). *Ultrason. Sonochem.* **2007**, *14*, 717–724.
- (6) Li, H.; Li, H. R.; Guo, Z. C.; Liu, Y. The application of power ultrasound to reaction crystallization. *Ultrason. Sonochem.* **2006**, *13*, 359–363.
- (7) Kresic, G.; Lelas, V.; Jambrak, A. R.; Herceg, Z.; Brncic, S. R. Influence of novel food processing technologies on the rheological and thermophysical properties of whey proteins. *J. Food Eng.* **2008**, *87*, 64–73.
- (8) Martini, S.; Potter, R.; Walsh, M. K. Optimizing the use of power ultrasound to decrease turbidity in whey protein suspensions. *Food Res. Int.* **2010**, *43*, 2444–2451.
- (9) Villamiel, M.; de Jong, P. Influence of high-intensity ultrasound and heat treatment in continuous flow on fat, proteins, and native enzymes of milk. *J. Agric. Food Chem.* **2000**, *48*, 472–478.
- (10) Martini, S. Chapter 2: An overview of ultrasound. In *Sonocrystallization of Fats*; SpringerBriefs in Food, Health, and Nutrition; Berlin, Germany, 2013; p 12.
- (11) Chow, R.; Blidt, R.; Chivers, R.; Povey, M. The sonocrystallisation of ice in sucrose solutions: primary and secondary nucleation. *Ultrasonics* **2003**, *41*, 595–604.
- (12) Chow, R.; Blidt, R.; Chivers, R.; Povey, M. A study on the primary and secondary nucleation of ice by power ultrasound. *Ultrasonics* **2005**, *43*, 227–230.
- (13) Patel, S. R.; Murthy, Z. V. P. Ultrasound assisted crystallization for the recovery of lactose in an anti-solvent acetone. *Cryst. Res. Technol.* **2009**, *44*, 889–896.
- (14) Patrick, M.; Blidt, R.; Janssen, J. The effect of ultrasonic intensity on the crystal structure of palm oil. *Ultrason. Sonochem.* **2004**, *11*, 251–255.
- (15) Higaki, K.; Ueno, S.; Koyano, T.; Sato, K. Effects of ultrasonic irradiation on crystallization behavior of tripalmitoylglycerol and cocoa butter. *J. Am. Oil Chem. Soc.* **2001**, *78*, 513–518.
- (16) Ueno, S.; Ristic, R. I.; Higaki, K.; Sato, K. In situ studies of ultrasound-stimulated fat crystallization using synchrotron radiation. *J. Phys. Chem. B* **2003**, *107*, 4927–4935.
- (17) Martini, S.; Suzuki, A. H.; Hartel, R. W. Effect of high intensity ultrasound on crystallization behavior of anhydrous milk fat. *J. Am. Oil Chem. Soc.* **2008**, *85*, 621–628.
- (18) Suzuki, A. H.; Lee, J.; Padilla, S. G.; Martini, S. Altering functional properties of fats using power ultrasound. *J. Food Sci.* **2010**, *75*, E208–E214.
- (19) Ye, Y. B.; Wagh, A.; Martini, S. Using high intensity ultrasound as a tool to change the functional properties of interesterified soybean oil. *J. Agric. Food Chem.* **2011**, *59*, 10712–10722.
- (20) Ye, Y.; Tan, C. Y.; Kim, D. A.; Martini, S. Application of high intensity ultrasound to a zero-trans shortening during temperature cycling at different cooling rates. *J. Am. Oil Chem. Soc.* **2014**, *91*, 1155–1169.
- (21) Chen, F. F.; Zhang, H.; Sun, X. Y.; Wang, X. G.; Xu, X. B. Effects of ultrasonic parameters on the crystallization behavior of palm oil. *J. Am. Oil Chem. Soc.* **2013**, *90*, 941–949.
- (22) Marangoni, A. G. On the use and misuse of the Avrami equation in characterization of the kinetics of fat crystallization. *J. Am. Oil Chem. Soc.* **1998**, *75*, 1465–1467.
- (23) Wright, A. J.; Hartel, R. W.; Narine, S. S.; Marangoni, A. G. The effect of minor components on milk fat crystallization. *J. Am. Oil Chem. Soc.* **2000**, *77*, 463–475.
- (24) Cheong, L. Z.; Zhang, H.; Xu, Y.; Xu, X. B. Physical characterization of lard partial acylglycerols and their effects on melting and crystallization properties of blends with rapeseed oil. *J. Agric. Food Chem.* **2009**, *57*, 5020–5027.
- (25) Meng, Z.; Liu, Y. F.; Jin, Q. Z.; Huang, J. H.; Song, Z. H.; Wang, F. Y.; Wang, X. G. Comparative analysis of lipid composition and thermal, polymorphic, and crystallization behaviors of granular crystals formed in beef tallow and palm oil. *J. Agric. Food Chem.* **2011**, *59*, 1432–1441.
- (26) Martini, S.; Herrera, M. L.; Hartel, R. W. Effect of cooling rate on crystallization behavior of milk fat fraction/sunflower oil blends. *J. Am. Oil Chem. Soc.* **2002**, *79*, 1055–1062.
- (27) Ishikawa, H.; Shiota, M.; Murakami, M.; Nakajima, I. Polymorphic behavior of palm oil and modified palm oils. *Food Sci. Technol. Int. Tokyo* **1997**, *3*, 77–81.
- (28) Sato, K.; Arishima, T.; Wang, Z. H.; Ojima, K.; Sagi, N.; Mori, H. Polymorphism of POP and SOS. I. Occurrence and polymorphic transformation. *J. Am. Oil Chem. Soc.* **1989**, *66*, 664–674.
- (29) Bayes-Garcia, L.; Calvet, T.; Cuevas-Diarthe, M. A.; Ueno, S.; Sato, K. In situ observation of transformation pathways of polymorphic forms of 1,3-dipalmitoyl-2-oleoyl glycerol (POP) examined with synchrotron radiation X-ray diffraction and DSC. *CrystEngComm* **2013**, *15*, 302–314.
- (30) Zhang, X.; Li, L.; Xie, H.; Liang, Z.; Su, J.; Liu, G.; Li, B. Effect of temperature on the crystalline form and fat crystal network of two model palm oil-based shortenings during storage. *Food Bioprocess. Technol.* **2014**, *7*, 887–900.